S1 Further information on the study site

Due to space limitations we were not able to include a photo of Langenferner in the paper. To impart a better image of the glacier we present Fig. S1 which is an aerial image of the glacier taken at the end of ablation season 2015.

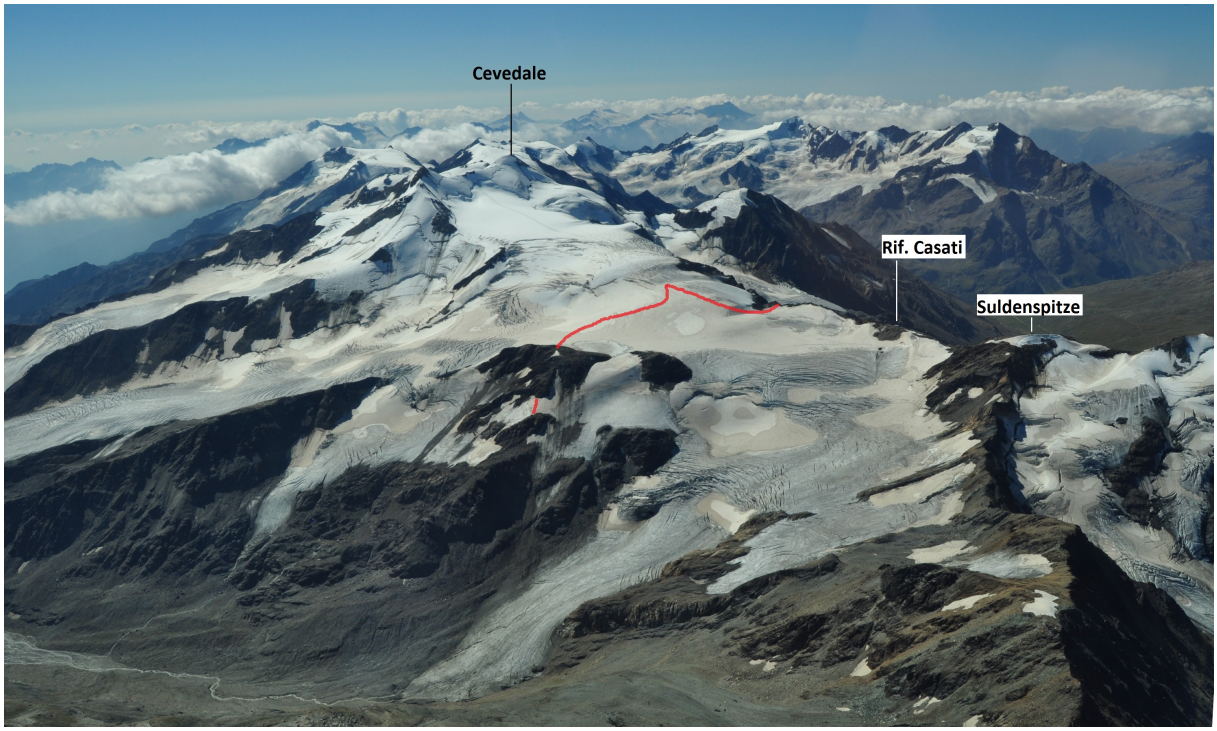

Figure S1: Aerial image of Langenferner taken by F. Covi on August 31^{st}, 2015. View direction is towards the South. The red line indicates the approximate location of the ice shed in the upper glacier part.

We also included Fig. S2 which is a map of Langenferner based on an orthophoto from the year 2008 provided by the Autonomous Province of Bozen / Südtirol. In this figure we show the locations of point measurements as used for the calculations of the annual mass balance 2013 since this information could not be shown in Fig. 2 of the paper. We also indicated debris cover which covers only small fractions of the glacier.

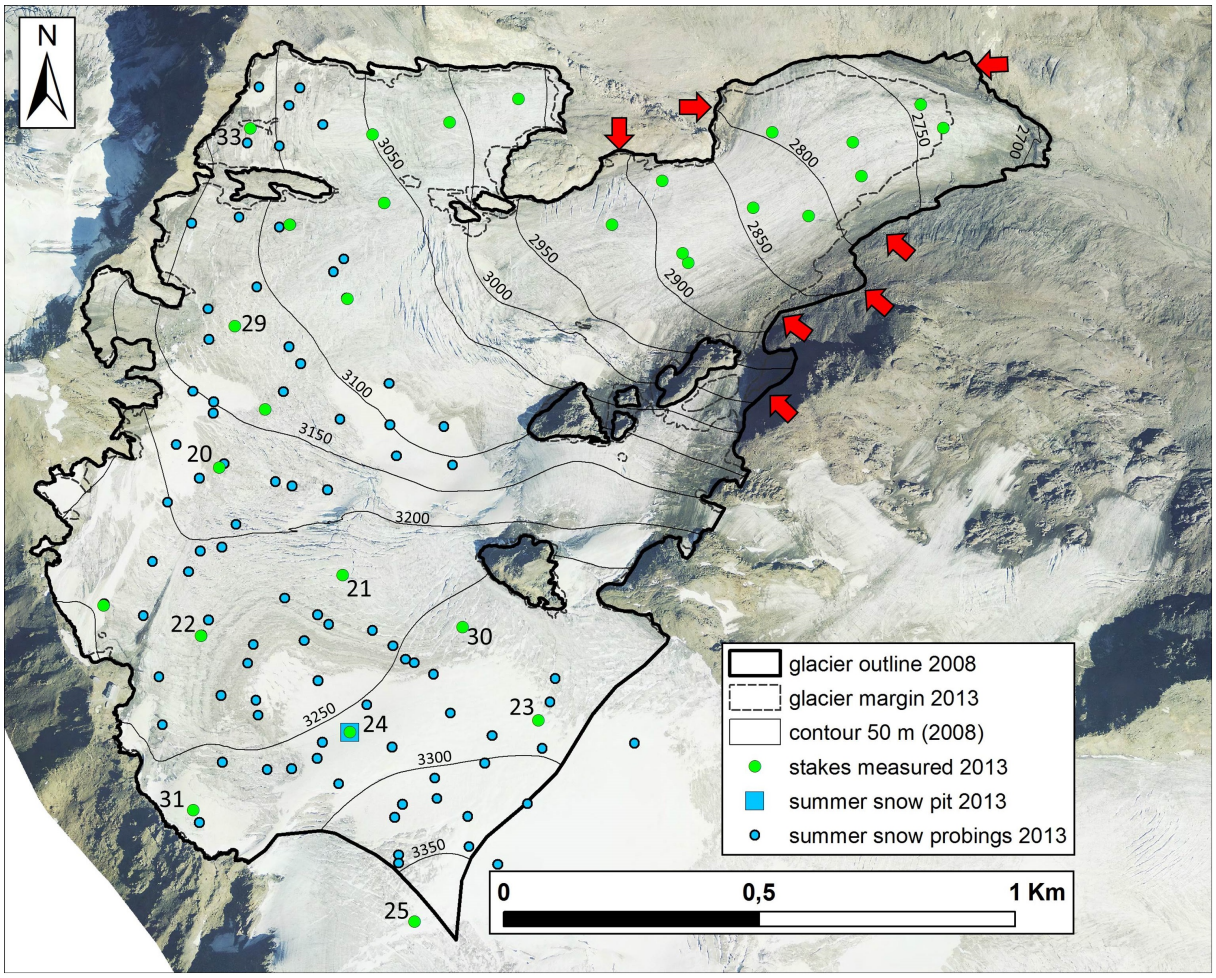

Figure S2: Map of Langenferner based on an orthophoto from summer 2008. The map shows the measurements used in the original and reanalysed calculation of annual mass balance in the year 2013. Red arrows indicate debris covered areas. Stake labels in the upper glacier part indicate the stake locations where the mass balance model was applied to.

S2 Homogenization of data

In this section we provide background information on the homogenization of the point data sets as used for the calculation of annual and seasonal mass balances. Figure S3 shows the point data consisting of snow pits and probings on which the reanalyzed series of winter mass balance is based.

S2.1 Winter mass balance - from floating date to fixed date

We calculated fixed date glacier wide specific winter mass balances by correcting floating date winter mass balance measurements for accumulation between the end of hydrological winter (April 30^th) and the date of measurements in early May (see Tab. S1) according to the description in the paper. In this correction we did not account for melting episodes. However, melt periods only have to be considered if the melt water leaves the glacier and is not retained in the snow pack (e.g. by refreezing in deeper layers). The presented correction method is hence only applicable to sites where no large amounts of melt water drain from the glacier during the period to which the correction is applied.
Normally no significant amounts of melt water drain from Langenferner in early May. Forthe study period this is supported by snow pits dug for winter balance measurements which indicate that the snow pack was never saturated with melt water, except for the extraordinary year 2007 when the snow pack in the lower glacier sections was saturated due to very warm weather in April. But even in that year no larger errors are expected from the correction method since in early May 2007 the weather conditions were cooler again. Apart from that, the reason for larger delays in measurements has always been unfavourable weather which in early May at altitudes of more than 2700 m (terminus of Langenferner) is commonly related to snow fall rather than significant melt. Table S1 shows the date when measurements for winter (and annual) balance were carried out and also shows the accumulation correction factor.

Table S1: Date of measurements for winter and annual balances and the correction factors used to convert floating date winter balances to fixed date balances.

year	winter balance	correction factor	annual balance
2004	May 14	0.8792	October 02
2005	May 02	1.0000	October 13
2006	May 12	0.8886	September 30
2007	May 10	0.9469	October 10
2008	May 09	0.9763	October 07
2009	May 07	1.0000	September 30
2010	May 18	0.8365	September 29
2011	May 04	0.9961	September 30
2012	May 08	0.9199	October 08
2013	May 14	0.9534	October 01

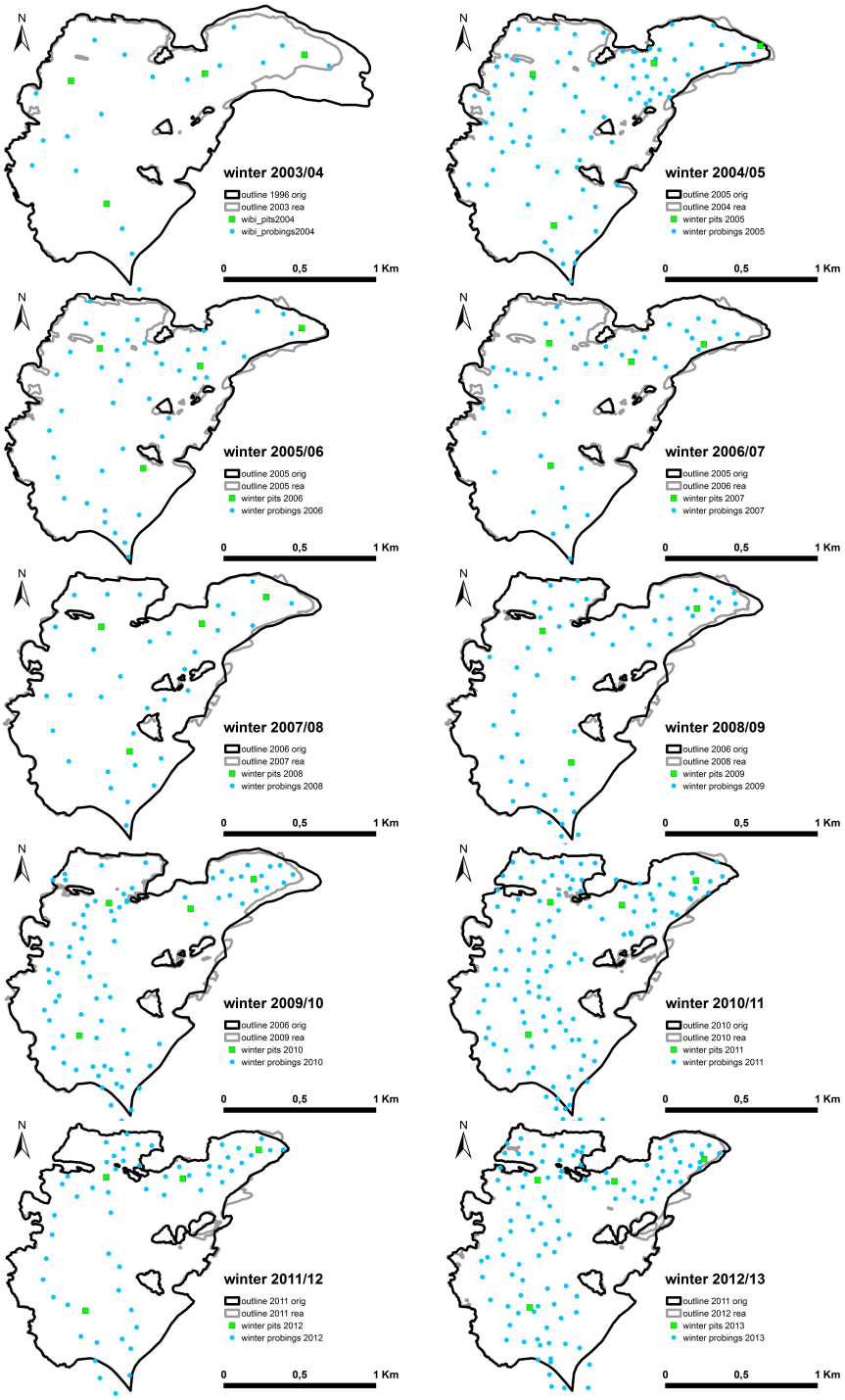

Figure S3: Point measurements as used to calculate the winter balances of all observation years. Original and reanalized winter balances differ due to differences in used outlines (orig versus rea), corrections applied to point measurements during the reanalysis and due to new extrapolation from point to glacier scale.

S2.2 Monte Carlo Optimization

The set of model parameters was optimized applying a Monte-Carlo model optimization performing 1000 runs for the period October 1^{st}, 2003 to September 30^{th}, 2013. The best model run was identified by validating the model results against readings at stake 22. Figure S4 shows the results of the 1000 model runs and the stake readings which were used to identify the best model parameter setting.

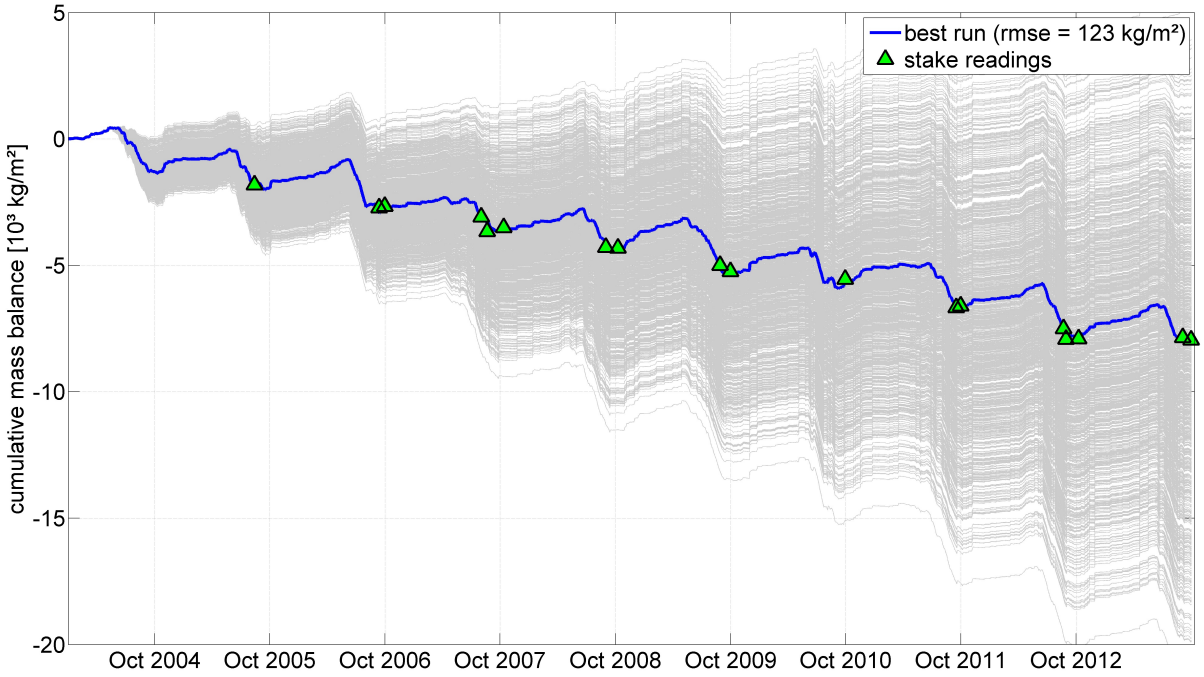

Figure S4: Cumulative mass balance series of the 1000 Monte-Carlo runs and measured cumulative mass balance at stake 22.

S2.3 Deriving the date of ice (or firn) emergence

The date of the emergence of the last years reference surface as shown in Tab. S2 was derived in a fully manual matter mainly from terrestrial, but also from aerial and space imagery. "Fully manual" here means that no automatic (and hence perfectly reproducible) algorithms were applied. First of all the images could not be geo-referenced and the location of stakes on the pictures was identified manually. Secondly, the choice of the emergence date was also done manually based on images from two different dates, one before the emergence and one after. This choice was based on meteorological conditions in the time period between the two image dates, as well as on site specific expert knowledge. The availability of continuous time lapse imagery would enable both, automatic geo-referencing of the images, as well as an exact and reproducible determination of snow line evolution. In presence of such data we expect a

further improvement of the skill of the applied model approach.

Table S2: Dates of melt of last winter snow as derived from terrestrial, aerial and space imagery.

Year	*Stake* 20	*Stake* 21	*Stake* 22	*Stake* 23	*Stake* 24	*Stake* 25	*Stake* 29	*Stake* 30	*Stake* 31	*Stake* 33
2004	08.03.	07.28.	08.05.	09.05.		08.05.	08.01.	08.13.	08.20.	08.10.
2005	07.04.	06.22.	07.20.	07.31.		06.25.	07.04.	07.17.	07.25.	07.30.
2006	07.20.	07.04.	07.20.	09.05.		07.15.	07.15.	07.20.	07.25.	07.25.
2007	07.18.	07.20.	07.23.	09.15.		07.31.	07.15.	07.29.	08.05.	08.01.
2008	07.06.	07.25.	08.10.	09.12.		08.15.	07.31.	08.06.	09.03.	08.05.
2009	08.09.	08.01.	08.10.			08.20.	08.05.	08.15.	08.29.	08.20.
2010	08.26.	07.05.	07.15.			07.16.	07.20.	08.28.		08.25.
2011	08.25.	08.05.	08.20.			08.20.	08.23.	08.23.	09.10.	08.25.
2012	08.05.	07.01.	07.25.	08.20.		07.01.	07.19.	07.25.	08.01.	08.01.
2013		08.05.	08.18.				08.13.			

S2.4 Point and year individual model tuning - the precipitation scaling factor Γ

In our study we apply a mass balance model with variable (in space and time) precipitation scaling. The role of the scaling parameter Γ is to account for local accumulation characteristics such as snow redistribution, which are strongly variable in space and time and are a priori unknown and independent from the characteristics at other (measured) stake locations. Although spatial characteristics show a to some extent re-occurring pattern in many years, even those can change due to special meteorological conditions. Statistical constraints would hence limit the allowed range of Γ which in turn would have negative impact on the model skill.
We see this tuning parameter as an "inverse model", allowing us to reconstruct the mass-balance from observations of the ice (or firn) emergence. While the primary goal of the paper is not to learn about physical processes behind glacier mass balance, the spatio-temporal variations of Γ indeed have a lot to say about them. Figure S5 shows Γ averaged over the study period (2004 to 2013) at the locations to which the model was applied. In the same figure we also added a colour coded map of the 2005 winter balance showing that high (low) values of Γ coincide with high (low) values of local winter mass balance.
Precipitation scaling factors (as shown in Tab. S3) were derived fitting the mass balance model to meet the observed /estimated date of the emergence of last year's reference surface (i.e. when the snow pack of the previous accumulation season has melted entirely). For some years and locations this was not possible, especially not for stake 24, which is located in a north exposed slope at an altitude of about 3270 m a.s.l. Even in years with very negative mass balance, this point may be subject to positive mass balance. Hence, the presented way of tuning the model did not work for this location. Nevertheless, mass balance information of this point was important for the reanalysis since no observations of that glacier part were available for the period 2004 to 2008. For that reason we calculated mass balances for this location applying the following procedure: First we calculated a series of "perfect Γ_i" for the years 2009 to 2013 by fitting the model to the measured mass balances $\pm$ 10 kg m^{-2} at this location. The same was done for the location of stake 31 which has a similar setting in terms of aspect and altitude

and is located only 300 m southwest of stake 24. We calculated a linear regression between the two series of relative anomalies of the resultant five-year series of Γ_i. This regression was subsequently used to derive relative Γ_i-anomalies for 2004 to 2008 at stake 24. Applying those to the average Γ_i of stake 24 (2009 to 2013) results in a complete series of Γ_i at stake 24 for the whole observation period.

Table S3: Precipitation scaling factors ($\Gamma_{i,a}$) used to model mass balance at stake locations.

Year	*Stake* 20	*Stake* 21	*Stake* 22	*Stake* 23	*Stake* 24	*Stake* 25	*Stake* 29	*Stake* 30	*Stake* 31	*Stake* 33
2004	2.0	1.7	1.8	2.7	3.4*	1.4	2.7	2.3	2.6	4.0
2005	2.0	1.3	2.3	2.6	2.3*	1.2	2.3	2.1	2.0	3.5
2006	3.0	1.6	2.8	3.6	3.0*	1.9	2.8	2.6	2.4	3.9
2007	2.9	2.6	2.6	3.1	2.8*	2.1	3.3	2.5	2.3	4.7
2008	1.8	1.9	2.8	3.6	4.3*	2.2	3.2	2.4	3.1	3.9
2009	2.6	2.1	2.4	3.2[1]	3.0[1]	2.0	2.7	2.3	2.4	3.6
2010	3.5	1.7	2.5	2.8[1]	3.8[1]	2.1	3.4	3.1	3.0[1]	4.2
2011	2.7	1.6	2.0	2.8[1]	2.5[1]	1.2	3.3	2.0	2.0	3.6
2012	3.8	1.6	2.6	4.2	3.5[1]	1.1	3.2	2.4	2.5	4.2
2013	2.8[1]	1.8	2.2	2.1[1]	2.6[1]	2.6[1]	2.7	2.3[1]	2.5[1]	3.3[1]
mean	2.7	1.8	2.4	3.1	3.1	1.8	3.0	2.4	2.5	3.9

[1] *perfect* $\Gamma_{i,a}$ (fitted to measured annual point mass balance), * $\Gamma_{i,a}$ derived from linear regression with Γ_i-series from nearby stakes.

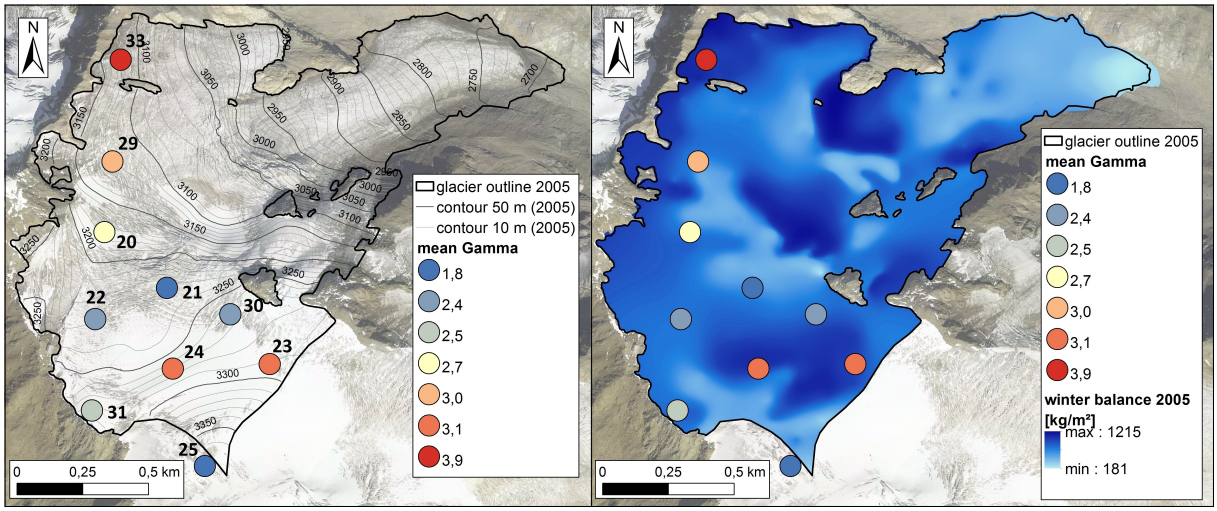

Figure S5: Color coded maps of mean Γ at the individual model locations during the study period. The left side figure is intended to give information on the local topography at individual locations which are labeled by stake numbers and the right side figure shows the mean gamma values in relation to measured winter mass balance of 2005.

S2.5 Validation of the mass balance model approach

While we present a scatter plot of modeled point balances versus measured ones in the paper, Tab. S4 shows the values for all modeled and measured annual balances. All 33 cases for which both modeled and measured balances are available were used to validate the applied model approach (Fig. 7 in the paper).

Table S4: Modeled and measured point mass balances.

Modeled										
Year	*Stake* 20	*Stake* 21	*Stake* 22	*Stake* 23	*Stake* 24	*Stake* 25	*Stake* 29	*Stake* 30	*Stake* 31	*Stake* 33
2004	−629	−1216	−763	−137	372*	−566	−1165	−506	−229	−866
2005	−1122	−1376	−694	−241	48*	−667	−1378	−699	−368	−880
2006	−901	−1544	−797	−157	−6*	−819	−1329	−736	−647	−841
2007	−1129	−1015	−889	−18	327*	−253	−1581	−583	−281	−908
2008	−1584	−1305	−779	−133	225*	−300	−1361	−785	−223	−1200
2009	−871	−1117	−789			−380	−1132	−623	−232	−601
2010	−90	−1002	−381			−133	−556	103		−218
2011	−782	−1428	−921			−801	−963	−731	−368	−916
2012	−992	−1776	−1206	−214		−1223	−1648	−1143	−825	−1383
2013		−421	−97				−356			
Measured										
2004										
2005										
2006										
2007	−1298	−1011	−881							
2008	−1799	−1288	−834			−323				
2009			−835	192	500					
2010	5	−979	−313	328	889		−611		350	−189
2011	−711	−1464	−1055	−364	106	−985	−834	−808	−278	−1101
2012	−819	−1949	−1300	−225	−51	−1602	−1873	−1265	−855	−1199
2013	184	−514	−15	380	707	113	−328	95	403	11

* $\Gamma_{i,a}$ derived from linear regression with Γ_i-series from nearby stakes.

S3 Glacier wide mass balance and extrapolation methods

In order to investigate uncertainties related to the extrapolation of point mass balances to the glacier wide scale, we applied a set of five different methods. The respective results for all individual years and seasons are shown in Tab. S5.

Table S5: Annual and seasonal glacier wide specific mass balances $[kg\ m^{-2}]$ calculated by different extrapolation methods. B_{ref} is the reference method, B_{orig} the original series, B_{clt} the traditional contour line method, B_{ptr} refers to point measurements extrapolated using *topo to raster*, B_{prm} represents the profile method, B_{ind} refers to inverse distance weighting, $range_{B_{rea}}$ is the range of all reanalysis methods (original results excluded) and $range_{B_{rea.bc}}$ is the same after bias correction. Bold values refer to numbers used as $\sigma_{glac.spatial.a}$ in the uncertainty analysis.

Annual

$Year$	B_{ref}	B_{orig}	B_{clt}	B_{ptr}	B_{prm}	B_{ind}	$range_{B_{rea}}$	$range_{B_{rea.bc}}$
2004	-1140	-1524	-1145	-1378	-1303	-1381	241	**28**
2005	-1456	-1233	-1460	-1750	-1658	-1749	294	**47**
2006	-1514	-1456	-1515	-1765	-1685	-1766	252	**23**
2007	-1539	-1616	-1541	-1719	-1604	-1676	180	**123**
2008	-1318	-1637	-1319	-1700	-1571	-1676	382	**134**
2009	-942	-998	-942	-1174	-1169	-1191	249	**55**
2010	-493	-659	-493	-664	-665	-674	181	**78**
2011	-1166	-1078	-1168	-1418	-1442	-1433	275	**87**
2012	-1556	-1532	-1559	-1810	-1711	-1786	254	**39**
2013	-246	-221	-247	-485	-449	-505	259	**24**

Winter

$Year$	B_{ref}	B_{orig}	B_{clt}	B_{ptr}	B_{prm}	B_{ind}	$range_{B_{rea}}$	$range_{B_{rea.bc}}$
2004	1022	1083	1021	976	927	961	**95**	68
2005	750	772	754	716	706	711	**48**	20
2006	925	1039	934	896	909	900	**38**	19
2007	558	642	554	530	547	515	**43**	33
2008	814	849	812	786	788	769	**45**	20
2009	1267	1343	1270	1265	1296	1273	**31**	56
2010	843	1076	839	820	787	795	**56**	29
2011	965	944	967	938	950	970	**33**	39
2012	932	995	944	892	910	903	**52**	29
2013	1216	1255	1215	1214	1204	1234	**31**	47

Summer

$Year$	B_{ref}	B_{orig}	B_{clt}	B_{ptr}	B_{prm}	B_{ind}	$range_{B_{rea}}$	$range_{B_{rea.bc}}$
2004	-2161	-2607	-2166	-2354	-2230	-2342	193	94
2005	-2206	-2005	-2214	-2466	-2363	-2460	260	38
2006	-2439	-2495	-2449	-2661	-2594	-2666	227	13
2007	-2096	-2258	-2095	-2249	-2152	-2191	154	126
2008	-2132	-2486	-2135	-2486	-2359	-2445	355	131
2009	-2211	-2341	-2212	-2439	-2464	-2464	256	95
2010	-1337	-1735	-1332	-1484	-1452	-1469	152	88
2011	-2132	-2022	-1235	-2401	-2392	-2403	271	100
2012	-2488	-2527	-2503	-2702	-2620	-2689	214	41
2013	-1462	-1476	-1462	-1699	-1652	-1739	277	60

S3.1 Representation of spatial mass balance patterns

For the reanalysis performed in the present study an extrapolation approach based on manually drawn mass balance contour lines was chosen as reference. This choice was based on the fact that the contour line method offers the best possibility to integrate additional expert knowledge such as snow line information or typical spatial patterns into mass balance analyses. Despite the problem of limited reproducibility, this method is - if applied thoroughly and in combination with a sufficient measurement set-up - still the most accurate. Figure S6 shows examples for contour lines as used for the calculation of Langenferners annual and seasonal mass balances in the year 2013.

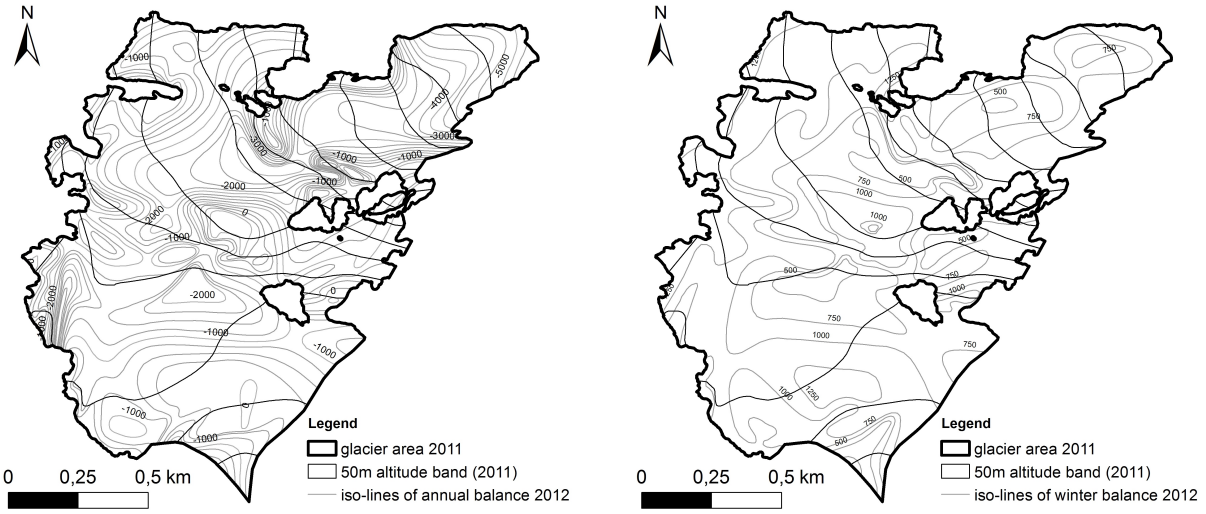

Figure S6: Manually drawn contour lines of 250 $kg\ m^{-2}$ equidistance for the annual and winter balance of 2012. Lines are based on point mass balances as presented in Fig. S2 and Fig. S3. For annual balances we also made recourse of information of the spatio-temporal snowline evolution as known from observations during the field campaigns in summer.

S4 Uncertainty assessment

S4.1 Uncertainties in glaciological mass balances

Uncertainty sources and respective values as applied in this study are shown in Tab. S6. For the uncertainty assessment, we assigned uncertainty values to each point measurement (stakes, pits, probings) individually as some of them are dependent on year and location. Tables with measurements and individual random uncertainty estimates are compiled in Supplement 2.

Table S6: Sources of uncertainties in annual glaciological mass balances at Langenferner as assumed for / calculated by the reanalysis.

point scale

source	**random**		**systematic**	
stake	reading error	0.03 m	tilted stakes (negative bias)	< 3%
	surface roughness	0.1 to 0.3 m		
snow pits	snow depth reading error	0.03 m		
	error in measurement of bulk density	15 kg m^{-3}		
	reference surface & snow corrections	50 kg m^{-3}		
snow probings	extrapolated snow density	20 kg m^{-3}	tilted probings (positive bias)	< 3%
	snow depth reading errors	0.02 m		

glacier scale

source	**random**		**systematic**	
stakes snow pits snow probings	propagation of point scale errors	9 to 26 kg m^{-2}	propagation of point scale errors	<2%
spatial integr.	inherent uncertainty of method	< 56 kg m^{-2}	can hardly be quantified ⇒ geodetic cross check	
reference area	uncertainties in glacier extent	< 20 kg m^{-2}	missing updates	<2%

Table S7 shows random uncertainty terms for individual years and seasons. The effect of point scale uncertainties on mean specific mass balances strongly depends on the amount of measurements since random errors cancel out each other if the number of measurements is large. The spatial distribution of measurements also plays a role. To test this we applied a bootstrap approach calculating each individual annual and seasonal mass balance 5000 times using the inverse distance method which was relatively easy to automatize. In each calculation a random error (according to a defined normal distribution corresponding to the assigned random uncertainty of the individual point) was added to each individual point measurement. The standard deviation of the 5000 resultant glacier wide mass balance values was then used as the random uncertainty related to point measurements. Uncertainties due to the extrapolation of point measurements were given by the term $range_{B_{rea.bc}}$ for annual and by $range_{B_{rea}}$ (see Tab. S5) for winter balance measurements. Uncertainties related to inaccurate glacier outlines are small in our study since we updated the glacier extent for each year. We estimated the remaining uncertainties of the reanalyzed series as ± 15 kg m^{-2} for all years except for the year 2004, for which we apply a more conservative estimate of ± 25 kg m^{-2} due to additional uncertainties in the glacier outline of that year. For winter balances the effect of inaccurate glacier outlines on mean specific balances is smaller due to small spatial gradients in winter balance.

Table S7: Random uncertainties in glaciological mass balances for glacier wide annual and seasonal mass balances. Overall number of used point balances N, number of modelled point balances N_{mod}, reanalized mass balance B_{ref}, random error related to propagated point uncertainties $\sigma_{glac.point.a}$, random error related to spatial extrapolations $\sigma_{glac.spatial.a}$, random error related to uncertainties in glacier area $\sigma_{glac.ref.a}$ and over all random uncertainty $\sigma_{glac.total.a}$.

Annual							
Year	N	N_{mod}	B_{ref}	$\sigma_{glac.point.a}$	$\sigma_{glac.spatial.a}$	$\sigma_{glac.ref.a}$	$\sigma_{glac.total.a}$
			$kg\ m^{-2}$	$kg\ m^{-2}$	$kg\ m^{-2}$	$kg\ m^{-2}$	kg m^{-2}
2004	32	10	-1140	25	28	15	41
2005	33	10	-1456	25	47	25	59
2006	30	10	-1514	26	23	15	38
2007	30	7	-1539	26	124	15	127
2008	32	6	-1318	22	134	15	136
2009	30	7	-944	24	55	15	62
2010	28	2	-493	18	78	15	82
2011	29	0	-1166	19	87	15	91
2012	28	0	-1556	23	39	15	47
2013	100	0	-246	11	24	15	31
mean	37	5	-1137	22	75	16	80
Winter							
2004	22	0	1022	16	95	5	97
2005	87	0	750	7	48	10	50
2006	47	0	925	10	38	5	40
2007	48	0	558	7	43	5	44
2008	36	0	814	10	45	5	46
2009	61	0	1267	14	31	5	34
2010	80	0	843	8	56	5	56
2011	127	0	965	7	33	5	34
2012	58	0	932	10	52	5	53
2013	109	0	1216	9	31	5	32
mean	68	0	929	10	50	6	52
Summer							
2004			-2161	30	99	16	105
2005			-2206	26	68	27	77
2006			-2439	28	45	16	55
2007			-2096	27	131	16	134
2008			-2132	24	141	16	144
2009			-2209	27	63	16	71
2010			-1336	19	96	16	99
2011			-2131	20	93	16	97
2012			-2488	25	65	16	71
2013			-1462	14	39	16	44
mean			-2066	25	90	17	95

S4.2 Uncertainties in geodetic mass balances

Uncertainties in geodetic mass balances are governed by the assumptions related to the conversion of observed volume changes to changes in mass, except for the period 2011 to 2013 when the effect of remaining uncertainties in the digital terrain models exceeds the uncertainties related to the density assumption. Table S8 shows the assumed random errors and their sources for the three geodetic balance periods of this study.

Table S8: Random uncertainties in geodetic mass balances.

Period	$B_{geod.corr}$	$\sigma_{geod.total}$	σ_{dc}	σ_{sc}	σ_{sd}	$\sigma_{geod.corr}$
	$kg\ m^{-2}$	$kg\ m^{-2}$	$kg\ m^{-2}$	$kg\ m^{-2}$	$kg\ m^{-2}$	$kg\ m^{-2}$
2005 - 2013	-9644	180	671	100	100	709
2005 - 2011	-7436	180	511	100	100	560
2011 - 2013	-2084	180	95	100	100	248